"Matrix" Effects in ToF-SIMS Analyses of Styrene−Methyl Methacrylate Random Copolymers[†]

X. Vanden Eynde* and P. Bertrand

Université catholique de Louvain, Unité PCPM, Place Croix du Sud 1,
1348 Louvain-la-Neuve, Belgium

J. Penelle

Department of Polymer Science and Engineering, University of Massachusetts,
Amherst, Massachusetts 01003-4530

Received November 22, 1999; Revised Manuscript Received April 27, 2000

ABSTRACT: Surfaces of several styrene (St)−methyl methacrylate (MMA) random copolymers have been analyzed by ToF-SIMS and XPS in order to detect any possible surface segregation of one of the two components and/or any specific matrix effect in the fragmentation processes. The observed O/(O + C) dependency on styrene content observed by XPS indicates that styrene−methyl methacrylate copolymers exhibit bulklike surfaces over the entire composition range of the copolymer. The absolute intensity of characteristic peaks from styrene or methyl methacrylate units was monitored by ToF-SIMS as a function of the styrene content. In positive mode, hydrocarbon fragments such as CH_3^+, $C_2H_3^+$, $C_2H_5^+$, $C_5H_5^+$, and $C_7H_9^+$ at $m/z = 15, 27, 29, 65$, and 93, respectively, decreased with increasing styrene content, while the intensities of MMA fragments decreased. All fragments exhibited intensity lower than that expected from a simple linear combination calculated from intensities associated with the MMA and St homopolymers. By contrast, some characteristic styrene peaks (such as $C_5H_3^+$, $C_7H_7^+$, $C_8H_7^+$, and $C_8H_9^+$ at $m/z = 63, 91, 103$, and 105, respectively) showed an absolute intensity higher than those observed for PSt and PMMA. In negative mode, fragments such as OH^- and C_2HO^- at $m/z = 17$ and 41 exhibited linear dependence with styrene content at the surface. Intensities for other MMA characteristic fragments such as $C_3H_3O^-$, $C_4H_5O_2^-$, $C_8H_{13}O_2^-$, and $C_9H_{13}O_4^-$ at $m/z = 55, 85, 141$, and 185, respectively, strongly decreased with increasing styrene content. These experiments as well as previous work on polystyrenes show that specific interactions between adjacent species take place during secondary ion emission, especially for the $C_7H_7^+$ fragment.

Introduction

Many crucial materials properties such as adhesion and biocompatibility are governed by the molecular state at the topmost surface.[1] As a result, techniques allowing quantitative polymer surface characterization are increasingly needed for both the characterization of existing materials and the design of new surfaces with well-controlled properties. Static secondary ion mass spectrometry (static SIMS) is one technique—among others—used to characterize polymer surfaces.[2−5] One of its main advantages resides in its higher surface sensitivity when compared to other techniques. The detection limit has been evaluated to be in the ppm concentration range, reaching the ppb level for some elements.[4] SIMS is able to distinguish quite easily the different molecular structures present on any polymer surface. Databases containing SIMS spectra of model compounds are becoming increasingly larger and provide considerable help in spectrum interpretation.[4] SIMS is sensitive among other factors to the polymer molecular structure,[6,7] branching,[6,7] cross-linking,[8] molecular weight,[9−11] tacticity,[12,13] and isomers.[14] The main drawback of SIMS is the difficulty in obtaining intrinsic quantitative relationships. The difficulty arises from the different and complex mechanisms induced by the collision cascade responsible for the secondary ion formation.[15−17]

Secondary ion generation for polymers containing the exact same repeat unit is dependent on different parameters. Experimental parameters are related to the primary ion source, in particular the nature, impact energy, incident angle, and charge state of the ion.[18−22] This point will not be discussed further as in all the experiments described here, all acquisition parameters were maintained constant. Other parameters are sample-connected and are solely related to the sample molecular structure and physical state when films are thick enough to minimize substrate effects.[23] All these sample-related effects are collectively considered in what is called the "matrix effects" (ME).[24,25] Matrix effects consider two possible cases, depending on whether the fragmentation of the repeat unit is dependent on long- or short-range specific interactions. In the former case (matrix effect of second type or MEII), interactions depend on neighboring functionalities that are not covalently attached on the polymer backbone (such as hydrogen bonding in some polymer blends),[26,27] while in the second case (matrix effect of first type or MEI), they depend on short-range interactions between adjacent covalently bonded functionalities such as in the specific rearrangements at end groups.[14] The long-range effect of hydrogen bonding between pyridine and phenol groups in a polymer blend has been observed in XPS and static SIMS spectra by Li et al.[26] Binding energy (BE) shifts in XPS and enhancement of some protonated

---

[†] Paper presented at the European Conference on Applications of Surface and Interface Analysis: ECASIA 99−Seville (Spain) in Oct 1999.

* Corresponding author. E-mail: vandeneynde@pcpm.ucl.ac.be.

10.1021/ma991960c CCC: $19.00

Scheme 1. Polymer Molecular Structures

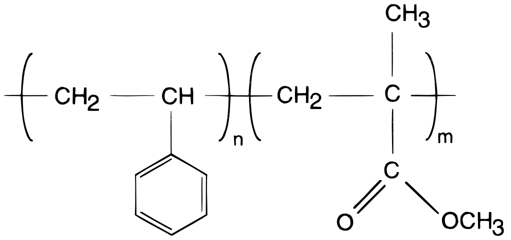

species in SIMS are related to the formation of hydrogen bonds in these blends. In our previous work, specific rearrangements due to short-range interactions (MEI) have been observed to occur at the polymer end groups of vinyl polymers.[14,28] Moreover, experiments on selectively deuterated polymers have shown that MEI is, in general, restricted to the directly adjacent functionalities.[29,30] Other experiments indicate that these short-range interactions should occur if a random distribution of two different units (M_1 and M_2 or M_1-*r*-M_2) can be achieved on the same macromolecular chain.[31,32] Such random distributions are typical of free-radical polymerization reactions and can be found in most vinyl copolymers obtained by a free-radical process.

SIMS characterizations of random copolymers have already been reported in the literature, but extracting relevant information on the unit contents, often based on the empirical selection of characteristic peaks, proved to be a difficult task.[33−49] Peaks have to be selected with extreme care. A study on poly(styrene-*r*-butadiene) showed for instance that intensity ratios of selected peaks can exhibit linear or nonlinear relationships with respect to the comonomer content.[42] A hidden assumption in the use of empirical relationships connecting peak intensities to monomer concentration is that peak relative intensities are directly proportional to the amount of repeat unit precursors present at the surface and that, as a consequence, matrix effects are negligible.[24] As it is known that matrix effects cannot always be neglected, it can be concluded that copolymer surface quantification based on SIMS data can only be achieved if peak intensities insensitive to neighboring functionalities can be identified in the spectra and/or the fragmentation pathways can be determined with accuracy. The purpose of this work was to analyze whether this might an achievable goal, starting from the styrene−methyl methacrylate copolymer.

To reach that goal, styrene−methyl methacrylate random copolymers (poly(St-*r*-MMA), Scheme 1) of known compositions were analyzed by XPS and SIMS. Surface compositions as obtained by XPS were used to interpret SIMS data. The absolute intensities of polystyrene (PSt) and poly(methyl methacrylate) (PMMA) characteristic fragments were monitored by SIMS as a function of the styrene content, making a direct interpretation of the SIMS results possible based on polymer fragmentation pathways.

Experimental Section

Samples and Film Preparation. Free-radical copolymerizations of styrene and methyl methacrylate were carried out in bulk at 80 °C using azobis(isobutyronitrile) (AIBN) as the initiator. Exact experimental conditions are provided in Table 1. The final polymer was obtained by precipitation in methanol at room temperature, filtered, and dried in an oven under vacuum. Exact copolymer compositions were determined by elemental analysis (Microanalysis Laboratory, University of Massachusetts) and quantitative ^{1}H NMR spectroscopy (Bruker 300 MHz, $CDCl_3$). Copolymerization kinetic parameters were computed with Prism software (2.0 Power PC Macintosh version) from GraphPad Software Inc.

Table 1. Experimental Conditions Used during the Copolymerization and Copolymer Bulk Charaterization[a]

ID code	reaction time (min)	styrene mole fraction in the feed (mol %)	styrene mole fraction in the copolymer (mol %)	
			NMR	elemental analysis
copo-70	15	79	71	70
copo-60	15	58	58	62
copo-46	30	35	45	47
copo-40	30	25	38	41

[a] General conditions: bulk, AIBN (0.67 mol %), 80 °C.

Each polymer was dissolved in benzene at a 30 mg/mL concentration (HPLC grade solvent from Union Chimique Belge, Belgium). A drop of this solution was spin-coated at 5000 rpm onto a silicon wafer (Wackers, Germany) used as received. The deposited films were then washed with *n*-hexane (Merck, Germany) in order to remove any residual contamination by poly(dimethylsiloxane) (PDMS) and quickly dried in air afterward. No further treatment was applied before analysis. Film depositions were made in a clean room atmosphere just before analysis. All samples were free of additives and low molecular weight compounds.

X-ray Photoelectron Measurements. The surface composition was quantitatively determined by XPS using a SSX 100 spectrometer (model 206, SSI, Surface Science Instrument) equipped with an aluminum cathode (10 kV, 11.5 mA) and a quartz monochromator. Surface compensation was obtained by using a low-energy (12 eV) electron flood gun and by covering the sample with a grounded nickel grid.

For each sample, a survey scan and detailed scans of O 1s and C 1s lines were performed with a 600 μm X-ray beam and a pass energy of 18 eV. The calibration of binding energy (BE) scale was made by setting neutral carbon (C−C and C−H bonds) peak at 284.7 eV for aromatic hydrocarbons and 285.0 eV for saturated ones. Other contributions to the core-level shift XPS spectra are listed latter in the text. A Shirley background subtraction was used, and peaks were synthesized by a least-squares routine using a set of Gaussian/Lorentzian (85/15) functions. Intensity ratios were converted into atomic ratios by using the sensitivity factors proposed by SSI (1 for carbon and 2.49 for oxygen atoms). No silicon signal from the substrate was ever observed in any XPS spectrum, implying that films are thicker than the XPS information depth of silicon (>10 nm) for all samples.

ToF-SIMS Analysis. Static SIMS measurements were carried out at UCL, Louvain-la-Neuve, with a Charles Evans & Associates TFS-4000 MMI time-of-flight spectrometer using a $^{69}Ga^+$ (15 keV) liquid metal ion source. Secondary ions were accelerated at 3 keV before being 270° deflected by three electrostatic hemispherical analyzers (TRIFT).[50] Secondary ions are accelerated up to 6 keV before entering the detector in order to enhance detection efficiency (especially at high m/z). A 880 pA dc primary ion beam is pulsed at a 11 kHz frequency with a pulse width of 23 ns bunched down to 4 ns for high mass resolution and is rastered over a 130 × 130 μm^2 surface area. All spectra were acquired with fluence $\approx 10^{12}$ ions cm^{-2} ensuring static conditions. A mass resolution $m/\Delta m$ of $\sim$ 4000 measured at $m/z = 28$ on a Si wafer was achieved. No charge neutralization was needed.

SIMS Data Treatments. All spectra treatments were made with the Cadence 2.0 software from Charles Evans & Associates. For each peak contributing to the spectrum (j), the absolute intensity $Y_{i,j}$ was measured and a unique ion composition (i) was assigned. As much as possible, metastable peaks were not added to the data.[51] Four spectra per polarity were acquired for each sample. Absolute intensity standard

Table 2. Sequence Length Distribution of MMA-(St)$_i$-MMA Fragments in the Random Copolymers

	probability (mole fraction)			
sequence length *i*	copo-40 (41 mol % St)	copo-46 (47 mol % St)	copo-60 (62 mol % St)	copo-70 (70 mol % St)
1	0.87	0.81	0.62	0.38
2	0.11	0.15	0.23	0.23
3	0.014	0.030	0.089	0.15
4	0.0018	0.0057	0.034	0.091
5	0.00023	0.0011	0.013	0.057
6	3.0×10^{-5}	0.00021	0.0048	0.035
7	3.9×10^{-6}	4.0×10^{-5}	0.0019	0.022
8	4.9×10^{-7}	7.6×10^{-6}	0.00069	0.014
total	0.9999	0.9999	0.9996	0.9772

Table 3. Sequence Length Distribution of St-(MMA)$_i$-St Fragments in the Random Copolymers

	probability (mole fraction)			
sequence length *i*	copo-40 (41 mol % St)	copo-46 (47 mol % St)	copo-60 (62 mol % St)	copo-70 (70 mol % St)
1	0.57	0.68	0.84	0.94
2	0.24	0.22	0.13	0.058
3	0.10	0.069	0.020	0.0036
4	0.045	0.022	0.0030	0.00023
5	0.019	0.0069	0.00047	1.41×10^{-5}
6	0.008	0.0022	7.17×10^{-5}	8.81×10^{-7}
7	0.0035	0.00069	1.10×10^{-5}	5.49×10^{-8}
8	0.0015	0.00022	1.69×10^{-6}	3.42×10^{-9}
total	0.9989	0.9999	0.9999	0.9999

deviations for characteristic peaks were about 10%. No silicon signal was observed.

Results and Discussion

Polymer Synthesis and Characterization. PSt and PMMA homopolymers were obtained from Polysciences Inc. (Warrington, USA) with molecular weights of 125 000 and 100 000, respectively. Copolymers used in this study were synthesized by bulk free-radical copolymerization of styrene (M_1) and methyl methacrylate (M_2) at 80 °C. Experimental conditions (Table 1) were designed to ensure low monomer conversions and make possible direct assessment of copolymerization kinetic parameters r_1 and r_2 from the experimental dependence of instantaneous copolymer composition on monomer feed composition. A computer-assisted statistical analysis of the experimental data by a nonlinear regression method was used to estimate r_1 and r_2. Such a statistical approach provides results of comparable or better quality than values obtained using classical linearization methods. Values of 0.44 and 0.25 were obtained for r_1 and r_2, respectively (standard errors: 0.04 on r_1 and 0.03 on r_2, $R^2 = 0.9986$). These numbers compare favorably to values from the literature.

Sequence-length distributions for MMA and St blocks up to the octad level were calculated from the experimental values of r_1 and r_2 and the feed composition of each copolymer. Final results can be found in Tables 2 and 3. The full statistical methodology allowing sequence-length distributions to be calculated from kinetic parameters in free-radical copolymerization is covered in several textbooks and will not be described here.[52]

The only assumption made in the statistical treatment of the experimental data is that the distribution of the comonomers along the polymer chain follows a first-order Markov statistical distribution (terminal model). Most experimental evidence accumulated in the literature suggests that this assumption is indeed correct in the case of styrene−MMA free-radical copolymerizations.[53] With the following kinetic parameters (k_d(AIBN) $= 104 \times 10^{-6}$ s^{-1}, $k_t = 6 \times 10^7$ M^{-1} s^{-1}, $k_p = 10^3$ M^{-1} s^{-1}, [AIBN] $= 7.2 \times 10^{-3}$ M, and [M] $= 9.35$ M), the degrees of polymerization were assumed to be about 100, and then copolymer molecular weights are about 10 000. Moreover, no signal from the AIBN initiator was observed in the NMR spectra and in the SIMS spectra (no $[C_4H_6N]^+$ peak present at *m/z* = 68.050).

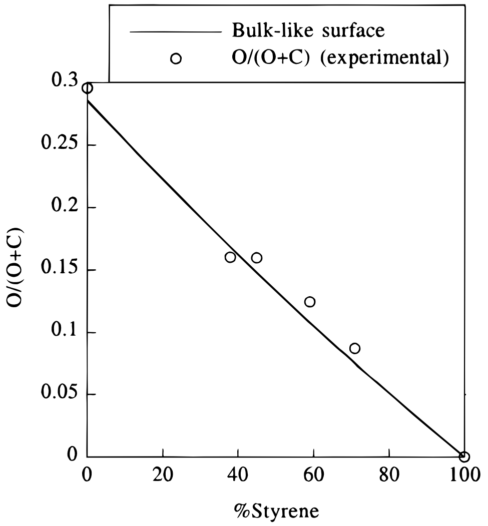

Figure 1. Oxygen ratio (O/(O + C)) of St-*r*-MMA copolymers as a function of styrene content. The continuous line is characteristic of a bulklike surface.

Surface Characterization by XPS. Surface composition was first characterized by XPS. Two contributions in the PSt C 1s core-level shift were observed: $\underline{\mathrm{C}}$−(C, H) at binding energy = 284.7 eV and the shake-up at BE = 291.2 eV. As expected, no oxygen signal appeared in the XPS spectrum of the polystyrene homopolymer. Four different contributions were found to be present in the PMMA C 1s core-level shift: $\underline{\mathrm{C}}$−(C, H) at BE = 285.0 eV, $\underline{\mathrm{C}}$−C(O)−O at BE = 285.8 eV, $\underline{\mathrm{C}}$−O at BE = 286.9 eV, and O=$\underline{\mathrm{C}}$−O at BE = 289.0 eV. C 1s core-level shifts varied with styrene content in the random copolymers, the observed signal being made of the overlap between XPS spectra of both homopolymers. Two components were observed in O 1s core level shift for MMA-containing polymers: C=$\underline{\mathrm{O}}$ at BE = 532.1 eV and C−$\underline{\mathrm{O}}$−C at BE = 533.7 eV. For all samples, the relative intensities of both oxygen components were equal, implying that no specific interactions appeared on the oxygen functionalities.

Figure 1 includes atomic ratios of oxygen (O/(O + C)) plotted as a function of the mole fraction in bulk styrene. It can be seen that the oxygen ratio decreases linearly from pure PMMA to pure PSt. The theoretical slope for a bulklike surface, i.e., same composition at the surface as in the bulk, is also indicated in Figure 1. The fact that experimental data are so close to the theoretical values indicates that, within experimental precision, styrene-*r*-methyl methacrylate copolymers present the same styrene content at their surfaces as in the bulk. This result is not as trivial as it first seems. It can be expected indeed that preferential localization of phenyl rings close to the surface, i.e., at the interface between the polymer and the vacuum, should occur in these copolymers due to the difference in surface energy associated with styrene and MMA units. It must be pointed out that the possibility of a slight increase in

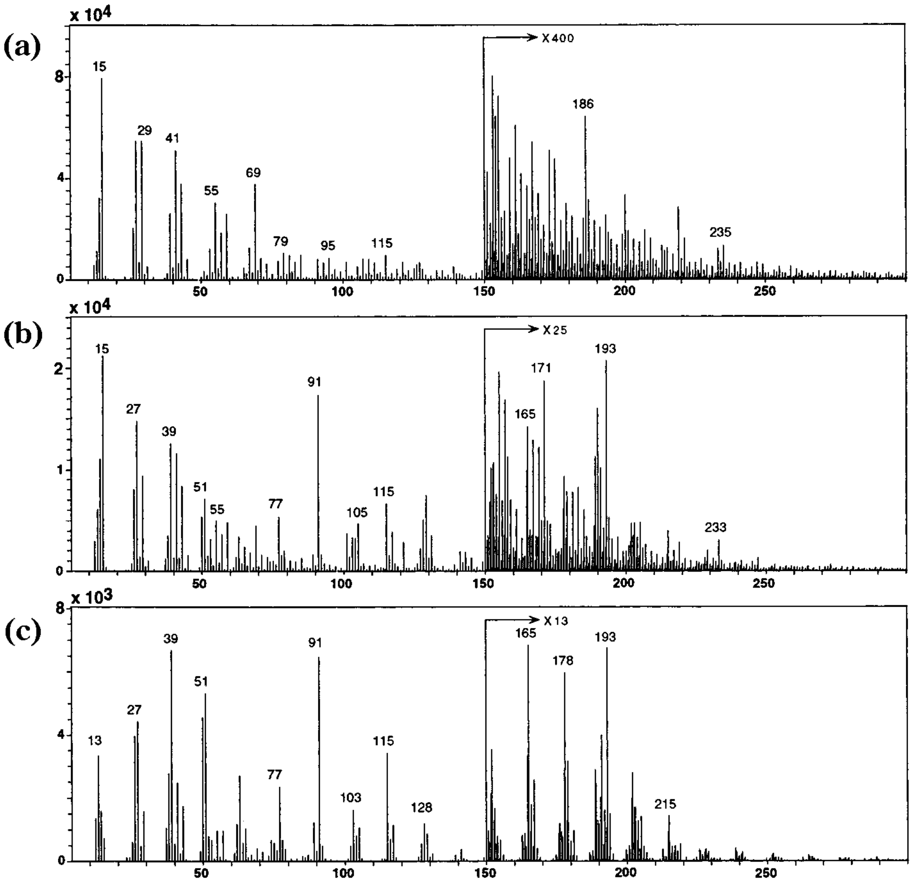

Figure 2. Positive SIMS spectra of (a) PMMA, (b) Copo-40, and (c) PS (m/z = 3−200).

local concentration cannot be entirely ruled out on the basis of our XPS data. Even if present, this reorientation of the surface cannot explain the differences in peak intensity variations observed in the second part of this study and can be considered to be very small and negligible at first approximation.

Polymer Surface Characterization by SIMS. A. Positive SIMS Spectra. **a. Styrene and Methyl Methacrylate Homopolymers**. Observed peaks on the PMMA SIMS spectrum (Figure 2a) are similar to those described in the literature.[54,55] Fragments associated with the MMA repeat unit ($C_5H_8O_2$) appears protonated ($C_5H_9O_2^+$) or results from the loss of an hydride ($C_5H_7O_2^+$) at m/z = 101 and 99, respectively. Other oxygen-containing peaks (as $C_4H_5O^+$, $C_7H_9O^+$ at m/z = 69 and 109) are characteristic of the main chain with the pendant group involved in their molecular structures. The methyl ester pendant group has also characteristic peaks at m/z = 15 (CH_3^+) and 59 ($C_2H_3O_2^+$). Branched hydrocarbon ions observed in the PMMA SIMS spectrum ($C_4H_5^+$, $C_4H_7^+$, $C_5H_7^+$, $C_5H_9^+$, $C_6H_7^+$, $C_6H_9^+$, $C_7H_9^+$, $C_7H_{11}^+$, and $C_8H_{11}^+$ at m/z = 53, 55, 67, 69, 79, 81, 93, 95, and 107, respectively) can be directly related to PMMA backbone fragmentation.[54] The SIMS spectrum of the polystyrene homopolymer is displayed in Figure 2c and shows typical carbon clusters. PSt SIMS spectra are mainly composed of hydrocarbon clusters with unsaturated and/or aromatic fragments ($C_2H_2^+$, $C_2H_3^+$, $C_3H_3^+$, $C_4H_3^+$, $C_5H_3^+$, $C_6H_5^+$, $C_7H_7^+$, $C_8H_7^+$, $C_8H_9^+$, $C_9H_7^+$, $C_{13}H_9^+$, and $C_{15}H_{13}^+$ at m/z = 26, 27, 39, 51, 63, 77, 91, 103, 105, 115, 165, and 193, respectively). Several authors determined the molecular structures of these ions with techniques such as isotopic labeling[56] and tandem mass spectrometry.[15,16]

b. Styrene−Methyl Methacrylate Copolymers. The SIMS spectrum of a copolymer (Copo-40) containing 38 mol % of styrene is also shown in Figure 2b, in direct comparison with the spectra of both homopolymers. It can be observed on one hand that, even at only 38 mol % of styrene in the copolymer, the styrene characteristic fragments are very intense when compared to most peaks associated with methyl methacrylate. This feature is clearly visible on peaks at m/z = 39, 51, 77, and 91. Other typical MMA peaks such as $C_2H_3O_2^+$ and [MMA−H]$^+$, at m/z = 59 and 99, also exhibit quite low intensities. This behavior is not general; however, other MMA fragments such as CH_3^+ and [MMA + H]$^+$, at m/z = 15 and 101, remain intense. It is interesting to note that no prominent peaks due to combined fragments of styrene and MMA units can apparently be observed on our SIMS spectra.

Our previous work on molecular-weight-dependent fragmentations established that total intensity is an important parameter for quantitative interpretation of SIMS data.[14] The total intensity (I_{tot}) of all ions is plotted in Figure 3 as a function of the styrene mole fraction in poly(St-*r*-MMA). It can be observed that I_{tot} is much larger for the MMA homopolymer than for the St homopolymer by a factor of ∼13 and that total intensities for St-*r*-MMA copolymers are below what would be expected on the basis of a simple linear combination of homopolymer contributions. These findings indicate that I_{tot} normalization procedures could lead to spurious variations and interpretations since such a procedure would involve two varying parameters.[24] As a result, only absolute intensities will be discussed in the following, except when specified.

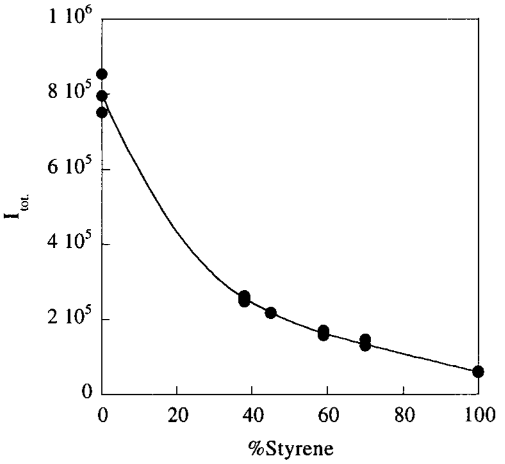

Figure 3. Positive total intensity ($I_{tot.}$) as a function of styrene concentration.

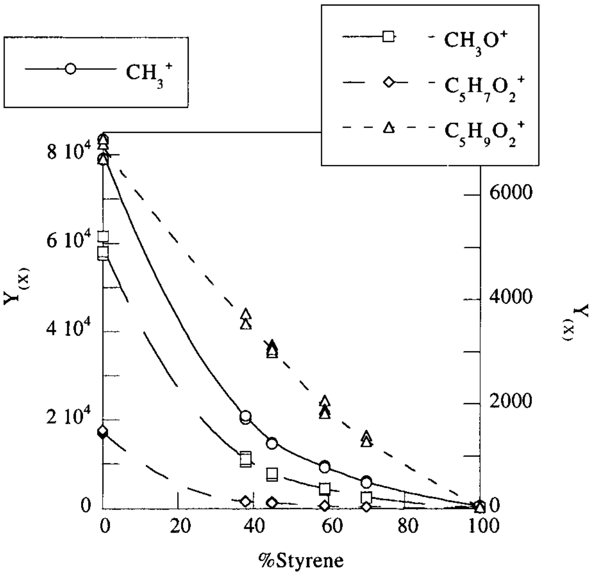

Figure 4. $Y(CH_3^+)$ and $Y(CH_3O^+)$ at $m/z = 15$ and 31 and protonated and deprotonated MMA unit peaks ($[M - H]^+$ and $[M + H]^+$ peaks are $C_5H_7O_2^+$ and $C_5H_9O_2^+$ at $m/z = 99$ and 101, respectively) are plotted as a function of styrene content in St-*r*-MMA.

Several peaks characteristic of PMMA and PSt were monitored as a function of the styrene mole fraction in poly(St-*r*-MMA). Evolution of signal intensity with styrene content was found to be very peak dependent.

Fragments from the PMMA fingerprint such as CH_3^+, CHO^+, CH_3O^+, $C_2H_3O_2^+$, $C_2H_5O_2^+$, $C_2H_3O^+$, $C_2H_5O^+$, $C_4H_5O^+$, and $C_4H_7O^+$ at $m/z = 15$, 29, 31, 55, 57, 43, 45, 69, and 71 (Figure 4 includes results for $Y(CH_3^+)$ and $Y(CH_3O^+)$ peaks), and $[MMA-H]^+$ or $C_5H_7O_2^+$ at $m/z = 99$ (Figure 4) shows a large decrease in intensity with styrene content, the signal being systematically lower than what would be expected on the basis of simple additivity. The evolution of each individual peak is slightly different as shown for example in Figure 4 for $Y(CH_3^+)$ and $Y(CH_3O^+)$. On the contrary, $[MMA + H]^+$ or $C_5H_9O_2^+$ at $m/z = 101$ (Figure 4) displays an evolution mostly linear with respect to styrene mole fraction.

Several aromatic fragments observed in the copolymer SIMS spectra can be related to the styrene unit. $Y(C_6H_5^+)$, $Y(C_7H_7^+)$, $Y(C_8H_7^+)$, and $Y(C_8H_9^+)$ are plotted in Figure 5 as a function of styrene content. Surprisingly, all these characteristic styrene fragments exhibit higher peak intensities for the copolymers than what would be expected on the basis of their composition. Their intensities are even higher than those observed for the homopolymers. For instance, $Y(C_7H_7^+)$ for the copolymer containing 38 mol % of styrene is multiplied by a factor ~3.3 and ~3.4 with respect to the signal for PMMA and PSt, respectively. It must be noted that the peak at $m/z = 115$ must be manipulated with great care as two different molecular ions contribute to the signal. These peaks at $m/z = 115$ are displayed in Figure 6 for both homopolymers and a copolymer. $C_9H_7^+$ is almost absent from the PMMA spectrum but not entirely as indicated by the presence of some metastable fragments.[51] Molecular structures for these interfering metastable ions are very difficult to determine. Nevertheless, it shows the almost complete disappearance of the oxygenated contribution at $m/z = 115$ for 38 mol % of styrene though any residual peak from the oxygenated fragments would be hidden by the $C_9H_7^+$ peak width.

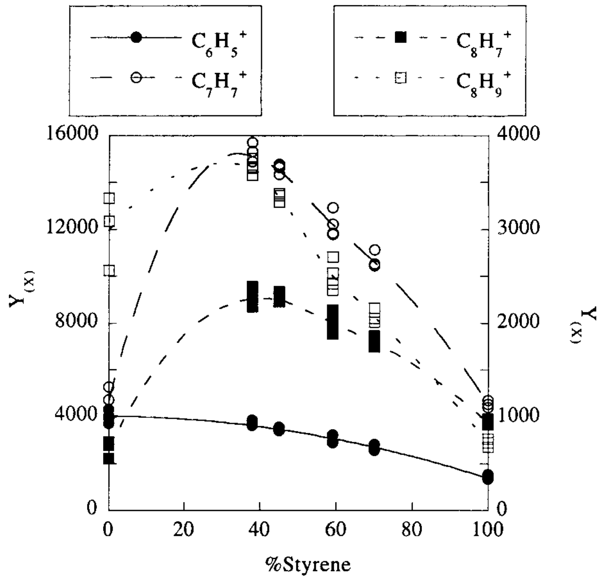

Figure 5. $C_6H_5^+$, $C_7H_7^+$, $C_8H_7^+$, and $C_8H_9^+$ as a function of styrene content in St-*r*-MMA.

It can be observed in Figure 5 that absolute intensities for the $C_7H_7^+$ ion, which is usually assigned to the tropylium ion, are similar for both homopolymers, meaning that the $C_7H_7^+$ molecular ion can be formed from either the styrene or methacrylate units with the exact same yields, but via two different pathways. The $C_7H_7^+$ ion can be formed from many hydrocarbon rearrangements or metastable decays close to the surface, and all the precursors for this ion have not been identified with certainty. Previous studies have shown that the $C_7H_7^+$ ion is generated from a styrene repeat unit but needs at least one hydrogen atom from the neighboring repeat units.[56] Styrene units have a H/C ratio equal to 1 whereas the MMA H/C ratio is 1.6 (counting all hydrogens, including those on the methyl ester). This higher hydrogen concentration for MMA units should improve the $C_7H_7^+$ formation from St units when only MMA neighbors are available. This is roughly what is observed experimentally: the $C_7H_7^+$ signal is much more abundant for copolymers than homopolymers. It seems reasonable indeed to assume that efficient mechanisms might exist to generate $C_7H_7^+$

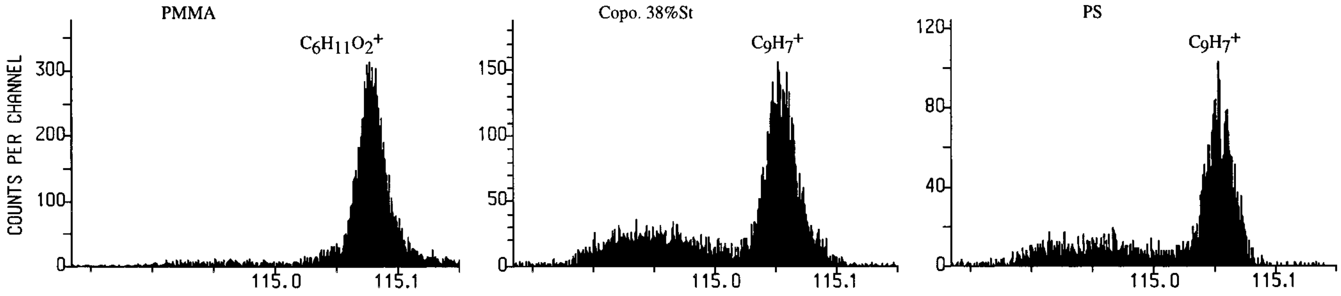

Figure 6. Positive SIMS spectra of PS, Copo-40 and PMMA (m/z = 115).

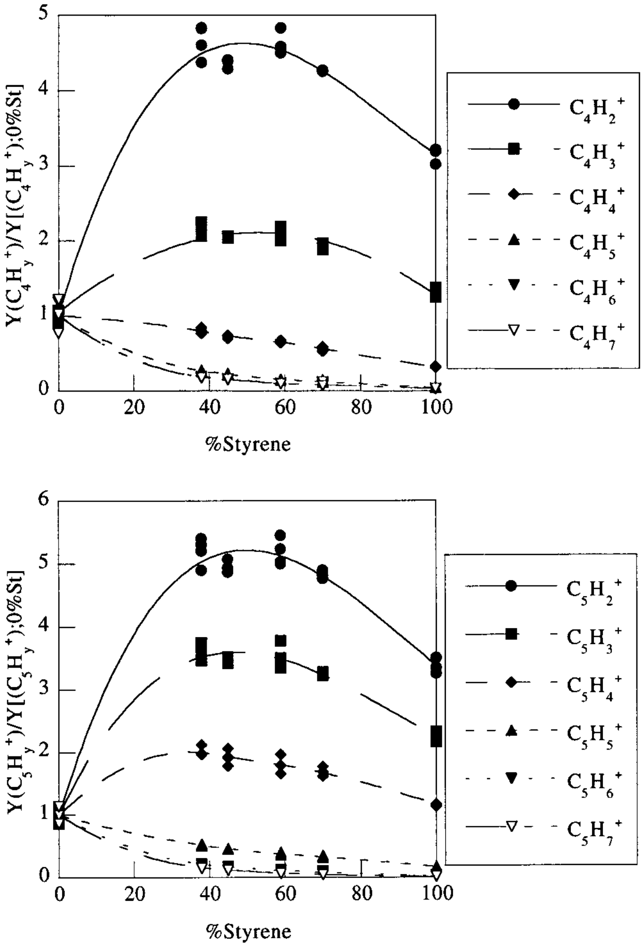

Figure 7. (top) C_4 and (bottom) C_5 hydrocarbon clusters as a function of styrene content in St-*r*-MMA. All the intensities were normalized to one for PMMA.

fragments by loss of neutral fragment like CO_2, H_2, or C_2H_2 from metastable ions of higher m/z.[15,16,51]

Intensity variations for two hydrocarbon clusters (C_4 and C_5) normalized with respect to the PMMA homopolymer signal are plotted in Figure 7 as a function of styrene content. Fragments with low hydrogen content exhibit behavior similar to $C_7H_7^+$ (shown in Figure 5) whereas those with high hydrogen content decrease as observed for most PMMA peaks (Figure 4). The transition from one regime to another varies with the hydrogen content in the fragment molecular structure, extreme behaviors being obtained in the C_4 (or C_5) series for $C_4H_2^+$ (or $C_5H_2^+$) and $C_4H_7^+$ (or $C_5H_7^+$). It has been observed previously that hydrocarbon peaks can be classified according to their hydrogen content and can describe systematic trends.[14,57,58]

B. Negative SIMS Spectra. Negative SIMS spectra for the homopolymers and a copolymer containing 38 mol % styrene are included in Figure 8. The spectra for the styrene and MMA homopolymers are comparable to those described in the literature.[4,54] In negative mode, fragments characteristic of the PMMA main chain are $C_3H_3O^-$, $C_4H_5O_2^-$, $C_8H_{13}O_2^-$, and $C_9H_{13}O_4^-$ at $m/z = 55$, 85, 141, and 185, respectively. The methyl ester pendant group is mainly characterized by a CH_3O^- peak at $m/z = 31$. O^- and OH^- ions are also present in the spectra and are directly related to MMA content in the macromolecule. Hydrocarbon fragments ($C_xH_y^-$) are emitted by both homopolymers. Like for positive SIMS spectra, no prominent peak containing combined styrene and MMA units could be observed in the spectra.

The total intensity (I_{tot}) is plotted in Figure 9 as a function of the styrene mole fraction in the St-*r*-MMA copolymers. A slight decrease in total intensity by a factor of about 1.3 appears between the two extremes (PMMA and PSt homopolymers). For the copolymers, I_{tot} seems to be slightly larger than expected on the basis of a linear contribution of each comonomer.

Several characteristic peaks were monitored as a function of styrene mole fraction (Figure 10). The intensity for low-mass fragments containing oxygen (O^-, OH^-, CHO^-, CH_3O^-, and C_2HO^- at m/z = 16, 17, 29 31, and 41, respectively) decreases linearly with styrene content in the copolymer. The other molecular secondary ions observed in PMMA decrease also but have their intensities below the expected linear relationship (Figure 11). The intensity of high-mass PMMA fragments involving several MMA units ($C_8H_{13}O_2^-$ and $C_9H_{13}O_4^-$ at m/z = 141 and 185) decrease more rapidly with styrene content than $C_3H_3O^-$ and $C_4H_5O_2^-$ at $m/z = 55$ and 85. $C_6H_5O^-$, $C_6H_6O^-$, and $C_6H_7O^-$ peak intensities at m/z = 93, 94, and 95, respectively, are plotted in Figure 12 as a function of the styrene content. Three different behaviors are observed for these ions with respect to the expected linear relationship: $C_6H_5O^-$ exhibits higher intensities while $C_6H_6O^-$ and $C_6H_7O^-$ peak intensities are lower, $Y(C_6H_6O^-)$ decreasing slower than $Y(C_6H_7O^-)$. Negative hydrocarbon ions appear in the spectra of both homopolymers. As in positive mode, observed behavior depends on the hydrogen content of the ion, but in the opposite direction. In the C_3 cluster (Figure 13), $Y(C_3^-)$, $Y(C_3H^-)$, and $Y(C_3H_2^-)$ (at m/z = 36, 37, 38 and 39, respectively) increase while $Y(C_3H_3^-)$ decreases with styrene content. No linear dependencies can be observed for these fragments.

Other parameters could interfere with the observed peak intensity behaviors as a function of the styrene mole fraction: trace of residual solvent and molecular weight of the copolymers. No trace of residual solvent could be observed in the SIMS spectra, in agreement

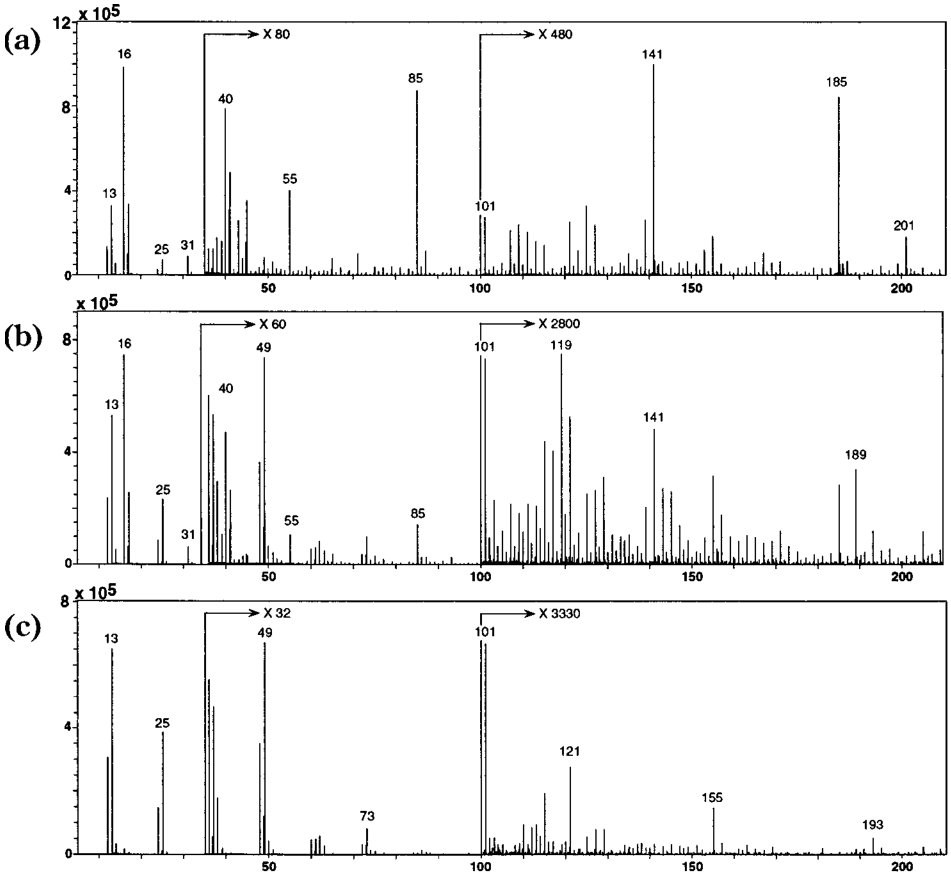

Figure 8. Negative SIMS spectra of (a) PMMA, (b) Copo-40, and (c) PS ($m/z = 3-210$).

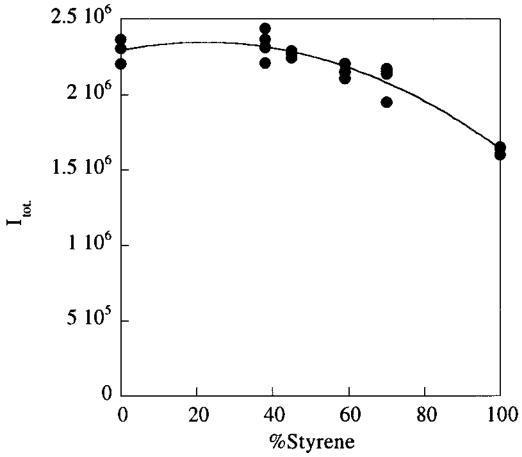

Figure 9. Negative total intensity as a function of styrene concentration.

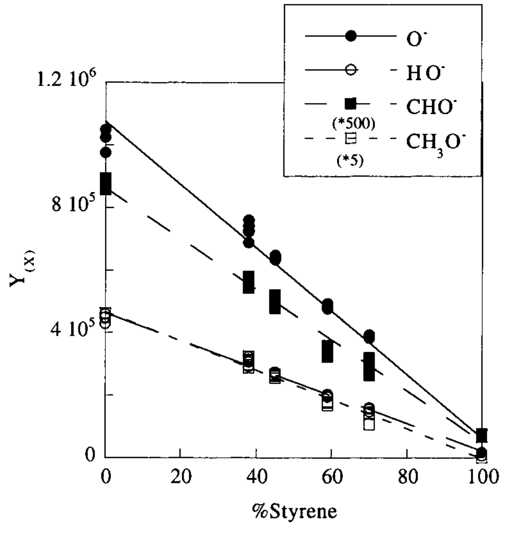

Figure 10. $Y(O^-)$, $Y(OH^-)$, $Y(CHO^-)$, and $Y(CH_3O^-)$ at m/z = 16, 17, 29, and 31 as a function of styrene concentration.

with results presented by Leeson et al.[55] These authors showed that, with the exception of THF, PMMA peak intensities are not influenced by the solvent (chloroform, 2-butanone, and toluene) used for the deposition. In the THF case, the molecule parent ion is observed in the SIMS spectrum. Deuterated polystyrene films deposited from toluene solution also did not exhibit contributions from the solvent.[58] Due to our experimental conditions, the copolymers exhibit lower molecular weights than homopolymers. It has already been shown in the literature that when molecular weight is decreased, the end group signals become prominent in the SIMS spectra, especially at low molecular weight.[14,57,58] Thus, this parameter cannot be excluded by the interpretation, but its influence in the experiments described in this paper seems to be minor. For instance, the $C_7H_7^+$ peak intensity, at $m/z = 91$, is increased by a factor of 1.5 when M_n is decreased from 10^5 to 10^4. (This factor is deduced from the molecular-weight-dependent fragmentations previously published in refs 14, 57, and 58.) By contrast, $Y(C_7H_7^+)$ is multiplied by 3.2 between homopolymers (PSt and PMMA) and copo-40 (Figure 5). In summary, the expected increase of characteristic peak intensities by changing the molecular weight from 10^5 to 10^4 cannot explain the major variations observed as a function of styrene mole fraction in the poly(St-*r*-MMA).

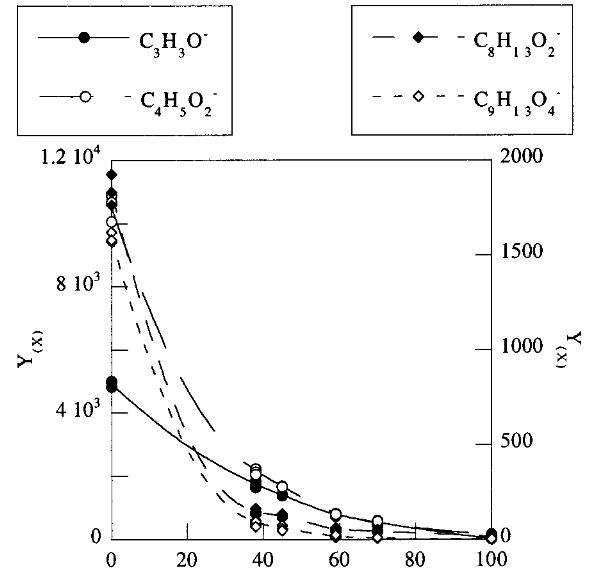

Figure 11. $Y(C_3H_3O^-)$, $Y(C_4H_5O_2^-)$, $Y(C_8H_{13}O_2^-)$, and $Y(C_9H_{13}O_4^-)$ at $m/z = 55$, 85, 141, and 185 as a function of styrene concentration.

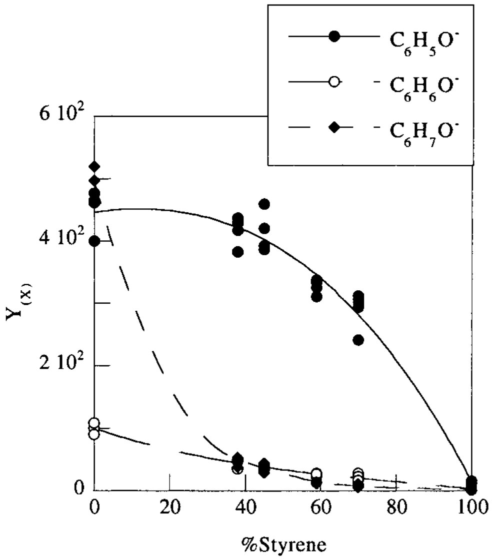

Figure 12. $Y(C_6H_5O^-)$, $Y(C_6H_6O^-)$, and $Y(C_6H_7O^-)$ at $m/z = 93$, 94, and 95, respectively, as a function of styrene concentration.

Identification of Useful Ions for Quantitative Characterization. Fragmentation pathways are much more complex in SIMS than in traditional mass spectrometry due to the additional factors associated with the surface macromolecular structure and morphology.[59] The characterization of a copolymer is even more difficult as the polymer chemical structure of the random copolymers increases significantly the number of theoretical precursors for a given molecular ion. Some significant trends can be drawn from our study on MMA-*r*-St copolymers.

A first important conclusion is that some oxygen-containing ion peaks (O^-, OH^-, and in a less perfect way CHO^- and CH_3O^-) exhibit linear relationships with respect to the comonomer content at the surface (as measured by XPS oxygen atomic ratio). No matrix effect seems to influence their fragmentation/ion formation pathways. We propose that these ions, being emitted by high-energy processes, can minimize the influence of structural factors on their emission yield. However, molecular fragments exhibit strong nonlinear relationships. PMMA characteristic fragments have intensities below what would be expected from MMA content in the copolymer and ion emission yield in the MMA homopolymer. By contrast, positive PSt fragments present intensity maxima at or below 38 mol % styrene. (The exact location of the maxima cannot be measured with certainty due to the lack of data in this concentration range.)

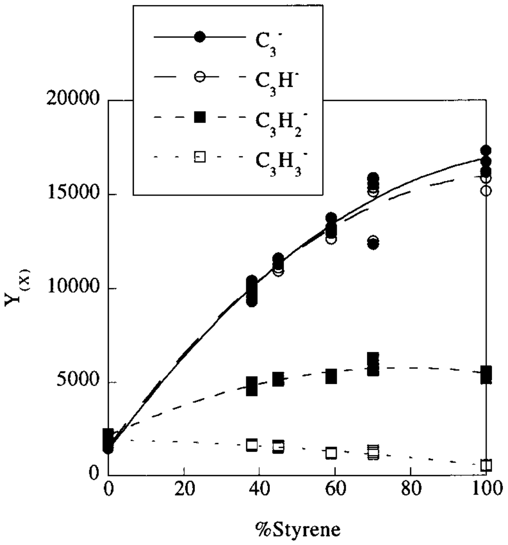

Figure 13. C_3 hydrocarbon cluster as a function of styrene content in St-*r*-MMA. All the intensities were normalized to one for PMMA.

High-mass secondary ions present in the PMMA spectrum exhibit strong decrease in intensity in poly(St-*r*-MMA) spectra, in particular at high styrene content. This behavior can be expected from the randomness of unit distributions in the polymer. As shown in Tables 2 and 3, $(MMA)_i$ segments in the copolymer chain have low probabilities that range from 25 to 6% at the diad level (two adjacent units) and from 11 to 0.4% at the triad level (three contiguous units).

As already discussed earlier in the case of the $C_7H_7^+$ ion, hydrogen transfer from styrene to MMA units seems possible for $[MMA + H]^+$, occurring at a similar probability as for transfer between adjacent MMA units. Similarly, $C_7H_7^+$ and most low hydrogen content and aromatic ions are enhanced by the presence of adjacent MMA units in the St-*r*-MMA chains. By contrast, the formation of $[MMA-H]^+$ is strongly inhibited by the presence of adjacent styrene units.

Difference in total secondary ion yields for PSt, poly(St-*r*-MMA), and PMMA samples are more substantial in positive than in negative acquisition mode. Polystyrene has a lower secondary ion yield than PMMA in both polarities, but the difference is much more significant in spectra obtained under positive rather than negative polarity. This change in the secondary ion emission yield is very important, in particular when trying to obtain quantitative data. Deviations with regards to the key parameter of interest for quantitative analysis—namely, the styrene content—indicate that normalization by this factor to obtain quantitative data is inadvisable.[24]

All our results on these random copolymers reemphasize the difficulty one has in SIMS when trying to identify the "most suitable" peak for quantitative work. Our study indicates that atomic ions might be the most appropriate to use to determine surface composition, although structural information is lost. Establishing a universal relationship allowing quantification based on molecular ions, while definitely more valuable, seems—on the basis of our present knowledge—to be behind what is presently feasible. Before such a goal can be reached, a better understanding on how the structural environment affects the emission yields of a functional group in a specific environment will have to be gained.

Conclusion

Surfaces of random styrene−methyl methacrylate copolymers (poly(St-*r*-MMA)) have been characterized by XPS and ToF-SIMS. Peak intensities were monitored as a function of the styrene content. XPS data indicate that copolymers present bulklike surfaces, irrespective of the comonomer composition. As expected, SIMS data are more complex to analyze. Most molecular secondary ions emitted from MMA units (such as $C_2H_3O_2^+$, $[M-H]^+$, $C_8H_{13}O_2^-$, and $C_9H_{13}O_4^-$ at $m/z = 59$, 99, 141, and 185, respectively) are inhibited by the presence of nearby styrene units, while some PSt fragment intensities are enhanced in the St-*r*-MMA copolymer (such as $C_7H_7^+$ and $C_8H_7^+$ at $m/z = 91$ and 103). New favorable pathways occur for their formation clearly due to the presence of surrounding MMA units.

Our present data confirm that prominent matrix effects play a major role in secondary molecular ion formation and/or emission from polymer targets, whatever the secondary ion polarity. Simple molecular ion intensity ratios are not directly useful for obtaining quantitative data from SIMS. Atomic or quasi-atomic secondary ions are much less sensitive to the polymer molecular structure, and direct quantitative relationships with sample content at the surface can be identified.

Without a much better understanding of fragmentation pathways, identification of useful molecular ions for quantitative work will be difficult. Studies on copolymers containing deuterated styrene or methyl methacrylate units or experiments on random copolymers with other molecular structures might help in approaching that goal and also give some new insights, by pinpointing specific fragmentation mechanisms.

Acknowledgment. Financial support from the "Fonds National de la Recherche Scientifique (FNRS)-Loterie Nationale" (Belgium) and from the "Région Wallonne" (Belgium) for the acquisition of the ToF-SIMS spectrometer is gratefully acknowledged. The Belgian Interuniversity Attraction Pole Program (PAI-IUAP P4/10) on "Reduced Dimensionality Systems" sponsored this work. The authors also thank the Unité de Chimie des Interfaces (CIFA, UCL) for access to the XPS spectrometer, as well as Lawino Kagumba, Joel Schall, Greg Dabkowski, and the PSE class of 1998 for their involvement in the synthesis and characterization of the copolymers.

References and Notes

(1) *Proceedings of 7th European Conference on Applications of Surface and Interface Analysis*; Olefjord, I., Nyborg, L., Briggs, D., Eds.; J. Wiley & Sons: Chichester, 1997.
(2) Vickerman, J. C.; Swift, A. J. In *Surface Analysis: the Principal Techniques*; Vickerman, J. C., Ed.; J. Wiley & Sons: Chichester, 1997.
(3) Briggs, D. In *Surface Analysis of Polymers by XPS and Static SIMS*; Clarke, D. R., Suresh, S., Ward, I. M., Eds.; Cambridge University Press: Cambridge, 1998.
(4) Vickerman, J. C.; Leggett, G. J.; Hagenhoff, B.; Briggs, D.; Chilkoti, A.; Bryan, S. R.; McKeown, P. J. In *Static SIMS Library;* Surface Spectra: Manchester, 1998.
(5) Bertrand, P.; Weng, L. T. In *Surface Characterization: A Practical Approach*; VCH Publishers: New York, 1997.
(6) van Ooij, W. J.; Brinkhuis, R. H. G. *Surf. Interface Anal.* **1988**, *11*, 430.
(7) Briggs, D. *Surf. Interface Anal.* **1990**, *15*, 734.
(8) van Ooij, W. J.; Mahmias, M.; Brown, A. *Surf. Interface Anal.* **1988**, *11*, 539.
(9) Reihs, K.; Voetz, M.; Kruft, M.; Wolany, D.; Benninghoven, A. *Fresenius J. Anal. Chem.* **1997**, *358*, 93.
(10) Galuska, A. A. *Surf. Interface Anal.* **1997**, *25*, 790.
(11) Vanden Eynde, X.; Bertrand, P. *Surf. Interface Anal.* **1998**, *26*, 579.
(12) Zimmerman, P. A.; Hercules, D. M. *Appl. Spectrosc.* **1994**, *48*, 620.
(13) Vanden Eynde, X.; Weng, L. T.; Bertrand, P. *Surf. Interface Anal.* **1997**, *25*, 41.
(14) Vanden Eynde, X.; Bertrand, P.; Jérôme, R. *Macromolecules* **1997**, *30*, 6407.
(15) Leggett, G. J.; Vickerman, J. C. *Int. J. Mass Spectrosc. Ion Processes* **1992**, *122*, 281.
(16) Leggett, G. J.; Vickerman, J. C.; Briggs, D.; Hearn, M. J. *J. Chem Soc., Faraday Trans.* **1992**, *88*, 297.
(17) Delcorte, A. Ph.D. Thesis, UCL, Louvain-la-Neuve, 1999.
(18) Hoshi, T.; Tozu, M.; Oiwa, R.; Zhanping, L.; Kudo, M. *Appl. Surf. Sci.* **1997**, *121/122*, 146.
(19) Galera, R.; Blais, J. C.; Blocbach, G. *Int. J. Mass Spectrom. Ion Processes* **1991**, *107*, 531.
(20) Stapel, D.; Brox, O.; Benninghoven, A. *Appl. Surf. Sci.* **1999**, *140*, 156.
(21) Briggs, D.; Hearn, M. J. *Vacuum* **1986**, *36*, 1005.
(22) Briggs, D.; Hearn, M. J. *Int. J. Mass Spectrom. Ion Processes* **1985**, *67*, 47.
(23) Delcorte, A.; Bertrand, P. *Surf. Sci.* **1998**, *412*−*413*, 97.
(24) Vanden Eynde, X.; Bertrand, P. *Appl. Surf. Sci.* **1999**, *141*, 1.
(25) Thompson, P. M. *Anal. Chem.* **1991**, *63*, 2447.
(26) Li, L.; Chan, C.-M.; Weng, L.-T.; Xiang, M.-L.; Jiang, M. *Macromolecules* **1998**, *31*, 7248.
(27) Coleman, M. M.; Painter, P. C. *Prog. Polym. Sci.* **1995**, *20*, 1.
(28) Vanden Eynde, X.; Oike, H.; Hamada, M.; Tezuka, Y.; Bertrand, P. *Rapid Commun. Mass Spectrom.* **1999**, *13*, 1917.
(29) Affrossman, S.; Hartshorne, M.; Jérôme, R.; Munro, H.; Pethrick, R. A.; Petitjean, S.; Vilar, M. R. *Macromolecules* **1993**, *26*, 5400.
(30) Affrossman, S.; Hartshorne, M.; Jérôme, R.; Pethrick, R. A.; Petitjean, S.; Vilar, M. R. *Macromolecules* **1993**, *26*, 6251.
(31) Painter, P. C.; Coleman, M. M. In *Fundamentals of Polymer Sciences*; Technomic Publishing: Lancaster, 1994.
(32) Kaim, A. *Macromol. Theory Simul.* **1997**, *6*, 907.
(33) Lub, J.; van Vroonhoven, F. C. B. M.; van Leyen, D.; Benninghoven, A. *J. Polym. Sci., Part B: Polym. Phys.* **1989**, *27*, 2071.
(34) Castner, D. G.; Ratner, B. D. *Surf. Interface Anal.* **1990**, *15*, 479.
(35) Briggs, D.; Ratner, B. D. *Polym. Commun.* **1988**, *29*, 6.
(36) Tomasetti, E.; Nysten, B.; Rouxhet, P. G.; Poleunis, C.; Bertrand, P.; Legras, R. *Surf. Interface Anal.* **1999**, *27*, 735.
(37) Galuska, A. A. *Surf. Interface Anal.* **1997**, *25*, 1.
(38) Galuska, A. A. *Surf. Interface Anal.* **1996**, *24*, 380.
(39) Galuska, A. A. *Surf. Interface Anal.* **1994**, *21*, 703.
(40) Brinen, J. S.; Rosati, L.; Chakel, J.; Lindley, P. *Surf. Interface Anal.* **1993**, *20*, 1055.
(41) Brinen, J. S.; Greenhouse, S.; Jarett, P. K. *Surf. Interface Anal.* **1991**, *17*, 259.
(42) Weng, L. T.; Bertrand, P.; Lauer, W.; Zimmer, R.; Busetti, S. *Surf. Interface Anal.* **1995**, *23*, 879.
(43) Leadley, S. R.; Davies, M. C.; Domb, A.; Nudelman, R.; Paul, A. J.; Beamson, G. *Macromolecules* **1998**, *31*, 8957.
(44) Chilkoti, A.; Castner, D. G.; Ratner, B. D.; Briggs, D. *J. Vac. Sci. Technol.* **1990**, *A8*, 2274.
(45) Affrossman, S.; Hindryckx, F.; Pethrick, R. A.; Stamm, M. In *First International Conference on Polymer-Solid-Interfaces*; Pireaux, J. J., Bertrand, P., Brédas, J.-L., Eds.; IOP Publishing Ltd: Bristol, 1992; p 337.
(46) Shard, A. G.; Volland, C.; Davies, M. C.; Kissel, T. *Macromolecules* **1996**, *29*, 748.

(47) Lianos, L.; Quet, C.; Duc, T. M. *Surf. Interface Anal.* **1994**, *21*, 14.
(48) Lang, F.-R.; Léonard, D.; Mathieu, H. J.; Moser, E. M.; Bertrand, P. *Macromolecules* **1998**, *31*, 6177.
(49) Davies, M. C.; Lynn, R. A. P.; Davis, S. S.; Hearn, J.; Watts, J. F.; Vickerman, J. C.; Johnson, D. *Langmuir* **1994**, *10*, 1399.
(50) Schueler, B. W. *Microsc. Microanal. Microstruct.* **1992**, *3*, 119.
(51) Delcorte, A.; Bertrand, P. *Int. J. Mass Spectrom. Ion Processes* **1999**, *184*, 217.
(52) Odian, G. In *Principles of Polymerization*, 3rd ed.; Wiley: Chichester, 1991; p 470.
(53) Frisch, H. L.; Mallows, C. L.; Bovey, F. A. *J. Chem. Phys.* **1966**, *45*, 1565.
(54) Hearn, M. J.; Briggs, D. *Surf. Interface Anal.* **1988**, *11*, 198.
(55) Leeson, A. M.; Alexander, M. R.; Short, R. D.; Briggs, D.; Hearn, M. J. *Surf. Interface Anal.* **1997**, *25*, 261.
(56) Chilkoti, A.; Castner, D. G.; Ratner, B. D. *Appl. Spectrosc.* **1991**, *45*, 209.
(57) Vanden Eynde, X.; Matyjaszewski, K.; Bertrand, P. *Surf. Interface Anal.* **1998**, *26*, 569.
(58) Vanden Eynde, X.; Reihs, K.; Bertrand, P. *Macromolecules* **1999**, *32*, 2925.
(59) McLafferty, F. W.; Turecek, F. In *Interpretation of Mass Spectra*, 4th ed.; University Science Books: Sausalito, 1993.

MA991960C